

D. Dewey, T.H. Markert, and M.L. Schattenburg

Center for Space Research
Massachusetts Institute of Technology
Cambridge, MA 02139

ABSTRACT

The design for a light-weight X-ray astronomical telescope that uses a diffractive optical element is described and simulated. The design provides tunable narrow-band imaging with a spatial resolution of several arc seconds over wide fields of view, greater than 10 arc minutes. The X-Ray energy range from 0.56 keV to 1.86 keV, containing astrophysically interesting lines of O, Ne, Fe, Mg and Si, would be covered with high throughput (200-1000 cm²) through the use of a blazed diffractive optic. State-of-the-art grating technology is adequate for the optic design and a variety of X-ray imaging detectors could be used for the readout.

Keywords: X-ray astronomy, X-ray spectroscopy, diffractive optics, diffraction gratings

1 INTRODUCTION

Recent years have seen the emergence of diffractive optics from a novelty to a key optic technology with devoted conferences^{1,2,3} and visibility in the trade press⁴. Given the narrow-band nature of many optical systems and the ability to fabricate structures with optical (500 nm) and suboptical scales this popularity is understandable.

But why would diffractive optics be viable in X-ray astronomy where wavelengths are short (*e.g.*, 1 nm), sources are polychromatic, and large collecting areas are required? The rest of this section summarizes the reasons and developments that are making a diffractive optic more feasible. Then, the following sections summarize the basic equations of a diffractive optic, discuss tilt-blazing for improved efficiency, and describe and simulate a specific “straw-man” diffractive-optic telescope system.

1.1 Motivation

Through our involvement in the fabrication and testing of the 336 grating facets that will make up the flight High Energy Transmission Grating, HETG,⁵ for the Advanced X-Ray Astrophysics Facility, AXAF, we are daily confronted with the fact that gratings can bend X-rays. In addition, the two-order of magnitude mass difference between the AXAF High Resolution Mirror Assembly, 1500 kg, and the comparable-active-area HETG, 12 kg, is glaring. These two observations have compelled us to look seriously at a diffractive optical system for X-ray astronomy.

There are other advantages to a diffractive optical system. Diffractive optics, “zones plates”, have very wide fields of view compared with Wolter-Schwartzchild optical systems.⁶ The tight alignment tolerances of reflective optics are removed and replaced by (more easily controlled) grating period tolerances in the diffractive system. A diffractive optical system can be designed to achieve arc second imaging which currently appears to be out of reach of light-weight foil mirror systems.

Of course there are disadvantages to which we apply the rule: “If you can’t fix it, feature it.”⁷ Thus the gross

Parameter	Diffractive optic	AXAF mirror	ASCA mirror
Effective area	1000 cm^2	1000 cm^2	325 cm^2
Field of view	> 10 arc min.	\approx 9 arc min.	12 arc min.
Angular resolution	< 5" HPD	1" HPD	170" HPD
Spectral range	0.5 - 1.9 keV	0.1 - 10 keV	0.5 - 12 keV
Spectral resolution	$E/dE \approx 500$	broadband	broadband
Key tolerance	period	figure, alignment	foil surface
Focal length	55-180 m	10 m	3.5 m
Weight	20 kg	1500 kg	9.8 kg

Table 1: Comparison of optics for X-ray astronomy. The example diffractive optic is compared with two “real-world” mirrors. The diffractive optic can fill the niche of low-weight, high angular resolution imaging.

chromatic aberration of a diffractive optical system suggests its use as a high resolution spectrometer. The long focal lengths for the system are an invitation to do without a cumbersome optical bench and mount the optic and detector on independent satellites.

Finally, as X-ray astronomy is entering a mature state, there is more room for instruments that fill niches rather than serve all uses. Table 1 shows a comparison of our example diffractive optic with the AXAF mirror and the ASCA foil mirrors.⁸ Clearly a diffractive optic has limitations but also advantages. Some examples of niches that a diffractive optic might fill are: i) narrow-band imaging of emission-line dominated extended sources, *e.g.*, super-nova remnants; ii) monitoring the time variability of lines in point sources; and iii) time-multiplexed spectral analysis of sources.

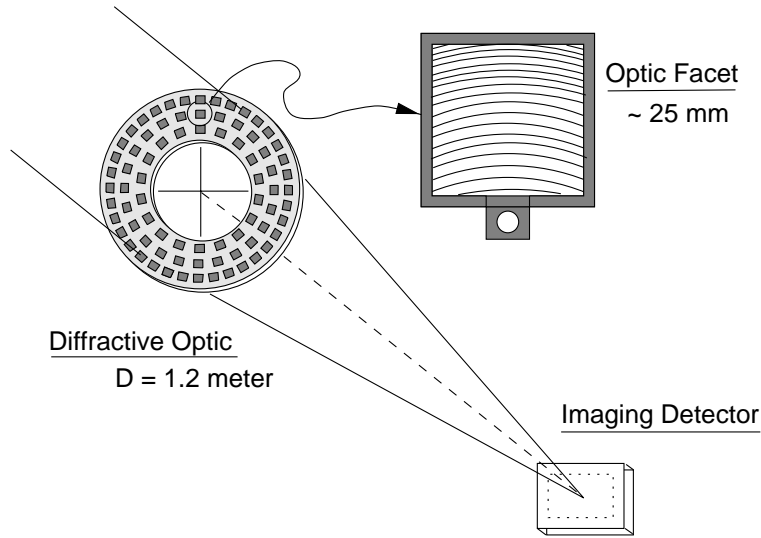


Figure 1: General concept for a faceted diffractive optic or “zone-plate telescope” for X-ray astronomy.

1.2 New Ideas

The motivating ideas above are now combined with some new ideas that enable a diffractive optic design. Chief among these is the ability to make fine grating periods (200 nm) with sufficient bar thickness to provide high diffraction efficiency.⁹ As will be seen below the finest period determines the F number of the optic.

With the physical reality of the HETG, the idea of a large-area “zone plate” made up from individual facets is much more tangible, Figure 1. This also leads to a design in which the grating bars are phase-coherent only on some sub-aperture scale. This is not unusual in the X-ray regime: the AXAF mirror angular resolution at $\lambda = 1$ nm corresponds to the diffraction limit from a 1 mm diameter region, three orders of magnitude below the optic’s physical diameter.

Another simplification in the diffractive optic is to use an open-center design. For example, if just the radial region from $0.7 r_{max}$ to r_{max} is filled with facets, then one-half of the available collecting area is used and yet the range of zone-plate periods varies by only $\sqrt{2}$. This is advantageous for the simplicity of the fabrication equipment and processes and for the test systems, *e.g.*, a single laser system could measure all periods. The open-center design also has an advantage for the instrument operation: out of focus radiation from an on-axis source is spread off-axis.

For a diffractive optic, only one of the two first orders is brought to a useful focus and for the simplest case of opaque zones this results in only 10% of the incident light forming the image. By using (tilt-)blazed transmission gratings, Section 3, it is now possible to get up to 30% of the light into the desired first order.

Past and planned advances in holographic techniques give confidence that suitably-patterned gratings can be fabricated to make up a diffractive optic. In particular, lessons have been learned in the issues of period fidelity and exposure-dose control and their effects on the grating product.

Finally, because the faceted diffractive optic design is azimuthally symmetric, only a limited number of facet types are required to fill the active area, one type populates each radial ring.

2 DIFFRACTIVE OPTIC THEORY

A general, insightful, and useful introduction to X-ray imaging systems and zone plates is given by Spiller.⁶ The specific status of diffractive optics for X-rays is reviewed by Michette¹¹ where the use of zone plates for microscopy is emphasized. He points out the use of a central stop and axial apertures to exclude other than the first order and he focuses on the water window, C K (0.28 keV) to O K (0.53 keV), where phase-blazed gratings can be made from Cr, Cu, Ni, and Ge. Finally, it is important to note that the general theory of zone plates¹² shows that they obtain an angular resolution equal to that of a comparable lens, *i.e.*, $1.22\lambda/D$.

Historically, it is interesting that a blazed diffractive optic was first used in a telescope at optical wavelengths by Wood almost a century ago.¹⁰ This zone plate was made with compass and ink on paper, photo-reduced and contact-printed into gelatine on glass producing a phase-blazed optic! Wood was able to use this optic to image craters on the moon at $f/50$.

The key design parameters for a diffractive optic can be chosen as: λ_0 , p_0 , and D ; as defined in Figure 2. The nominal wavelength, λ_0 , sets, of course, the wavelength range of interest and, importantly, dictates the type of optical materials that are available to make the diffractive element. The finest grating period, p_0 , is generally determined and limited by the available fabrication technology. Finally, the optic diameter, D , determines the collecting area and sets the scale for the size of the telescope. For reference, nominal values of these three parameters for the present application are: $\lambda_0 = 1$ nm, $p_0 = 200$ nm, and $D = 1.2$ m.

The starting point for diffractive optics from a grating perspective is the deflection angle produced by a diffraction grating given by the grating equation:

$$\sin \theta_i + \sin \theta_d = \frac{m\lambda}{p} \quad (1)$$

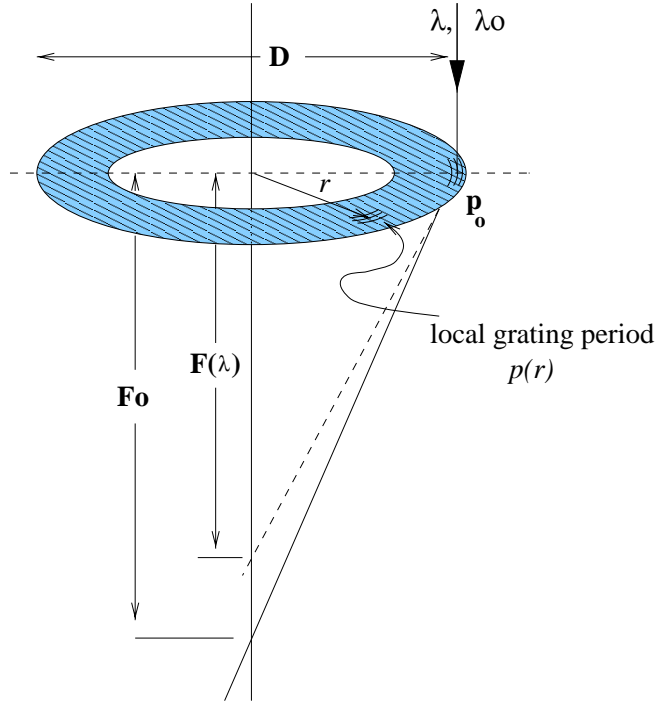


Figure 2: Definition of diffractive optic geometry. The key design parameters are the nominal wavelength, λ_0 , the extreme period, p_0 , and the optic diameter, D . The local period is a function of radius and is chosen so that parallel rays of wavelength λ_0 come to a common focus at $F_0 = F(\lambda_0)$.

where θ_i and θ_d are the angles of incidence and diffraction, p is the period of the grating, and m is the diffracted order. Considering generally the case $m = 1$, the F number of the diffractive optic, defined as the ratio of focal length to entrance pupil diameter,¹³ is determined by the wavelength and the extreme period:

$$F \text{ number} = \frac{1}{2} \sqrt{\frac{p_0^2}{\lambda^2} - 1} \approx \frac{p_0}{2\lambda}; \quad (2)$$

and the focal length of the system is:

$$F(\lambda) = \frac{D}{2} \sqrt{\frac{p_0^2}{\lambda^2} - 1} \approx \frac{Dp_0}{2\lambda}. \quad (3)$$

Using the nominal parameter values in these equations gives an F number of $f/100$ and a focal length, $F(\lambda_0) = 120$ m.

The design of the optic involves choosing the period as a function of off-axis location so that parallel monochromatic rays are focussed to a point. This results in the requirement that:

$$p^2(r) = \left(\frac{r_{max}}{r}\right)^2 p_0^2 - \lambda_0^2 \left[\left(\frac{r_{max}}{r}\right)^2 - 1\right] \quad (4)$$

where $r_{max} = D/2$. Owing to the large F number of the systems here the resulting optic is only weakly “tuned” and works well for a range of wavelength.

3 OPTIC EFFECTIVE AREA

The effective area of the objective is given by:

$$A_{eff} = \eta_{diff}(\lambda)\eta_{geom} \frac{\pi D^2}{4} \quad (5)$$

where η_{geom} is the fraction of the circular area that is covered with active diffractor and $\eta_{diff}(\lambda)$ is the first-order diffraction efficiency of the grating structure. Filling 1/2 of the optic geometric area and including an additional factor of 0.7 for mounting hardware, a reasonable value for η_{geom} would be 0.35.

Through the use of blazed transmission gratings single-sided diffraction efficiencies, $\eta_{diff}(\lambda)$ approaching 30% can be realized. The ideal blaze profile for a transmission diffraction grating has an asymmetric, roughly saw-tooth, shape.¹¹ Current fabrication technologies may more conveniently provide symmetric bar shapes. In this case the required blaze profile can then be obtained by using the gratings at a fixed off-normal tilt angle.¹⁴ Figure 3 shows the efficiency vs. energy for such a “tilt-blazed” grating. The resulting effective area for the nominal optic design is shown in Figure 4 and approaches 1000 cm². A polyimide support layer, as in the HETG gratings, is included.

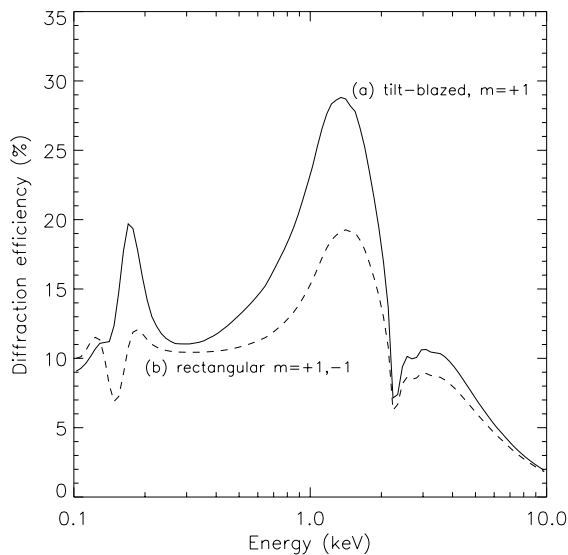


Figure 3: Comparison of tilt-blazed grating and rectangular-phased grating models, each optimized at 1.2 keV. (a) the $m = +1$ efficiency for a tilted trapezoidal grating (period = 200 nm, grating bar base width of 140 nm, bar height of 350 nm, side-wall slopes of 9 degrees, and operated at a 9 degree angle of incidence.) (b) the efficiency for each first order of a rectangular grating (period = 200 nm, grating bar width of 100 nm, bar height of 280 nm, and operated at normal incidence.) The grating bars are made of gold and no support structure effects are included.

4 SPECIFIC DEMONSTRATION DESIGN

4.1 Diffractive Optic Design

An optimum zone plate design requires that the local grating period and angle vary. Given the need for a large collecting area for astronomical use of the optic and the resulting long focal length and large focal plane

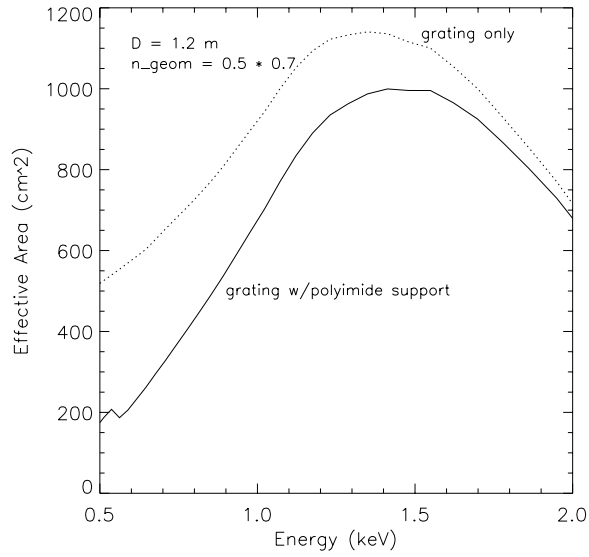


Figure 4: Resulting effective area for the diffractive optic design with optic parameters $p_0 = 200$ nm, $\lambda_0 = 1$ nm, and $D = 1.2$ m. The effect of an $0.5 \mu\text{m}$ polyimide support layer is indicated.

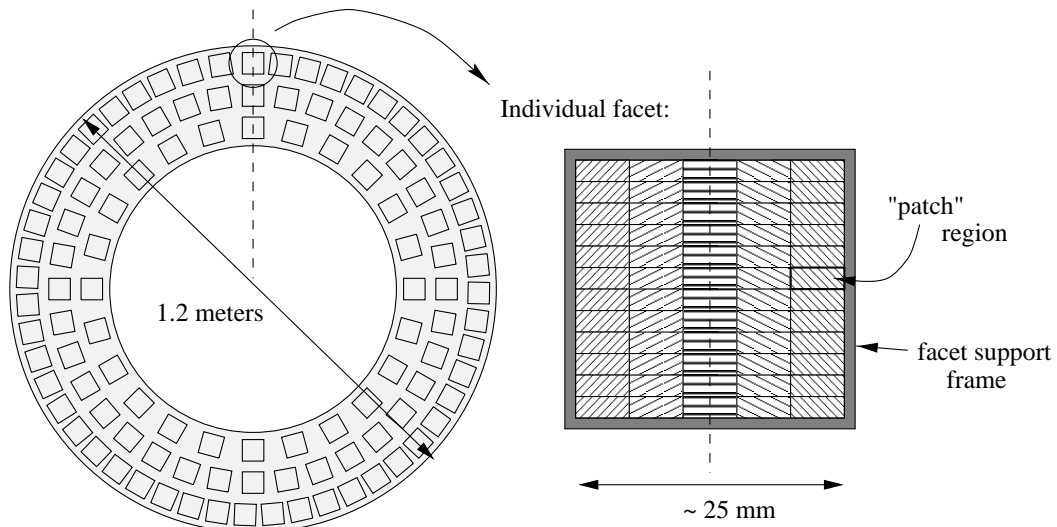


Figure 5: Schematic design of the diffractive optic. The active area of the 1.2 meter aperture is tiled with rings of facets. All facets at the same radius are identical. At right, the “patched” nature of the facets is displayed. Each patch region has a unique period and grating-line orientation.

spot size (≈ 0.5 mm) it is reasonable to consider a discrete approximation to the zone plate, Figure 5. The optic is made up from a collection of facets of reasonable physical size, e.g., 25×25 mm. The facets each have the required zone-plate pattern but the pattern is simplified through the use of patches where the period and grating-line orientation are locally constant. This represents a very conservative expectation on the ability to fabricate zone-plate-like structures.

In general, such a faceted design allows an additional design degree-of-freedom: the diffractive optic surface may have a non-planar, rotationally symmetric shape.¹⁶ However, for high F number systems (as in this X-ray region) the planar design is very close to optimum and so the facets are all in a plane as in a classic zone plate.

4.2 Resolution of the “patched” Design

The design decision to make the diffractive optic from patches of constant-period, parallel grating lines, sets the imaging quality of the telescope. This represents the extreme case where the sub-apertures provide no focussing power. The image is formed conceptually as the superposition of the projections of all the patches, as shown in Figure 6.

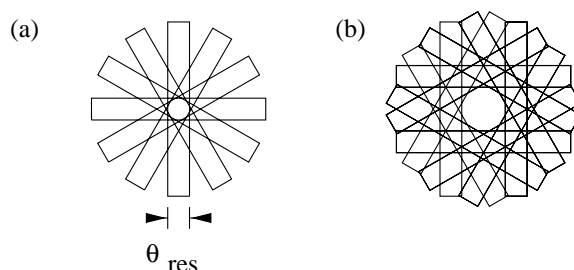


Figure 6: *The formation of the image due to the patched gratings. (a) the image is in focus and the centers of the patches’ images are coincident. (b) the image is defocussed (detuned) slightly producing a radial shift of the patches by 1.5 times the patch width.*

For this faceted design choice there is an optimum facet width, w_{opt} , which balances the image size due to the patch size and the image size due to diffraction:

$$w_{opt} \approx F_0 \frac{\lambda_0}{w_{opt}} \implies w_{opt} = \frac{1}{\sqrt{2}} \sqrt{Dp_0} \quad (6)$$

This leads to a minimum imaged width of the patches of $w_{image} \approx \sqrt{2}w_{opt} = \sqrt{Dp_0}$ and to an angular resolution of

$$\theta_{res}(\lambda_0) = \frac{2\lambda_0}{\sqrt{Dp_0}} \quad (7)$$

For our nominal parameters this corresponds to 0.84 seconds of arc and a patch width of 0.35 mm. In practice the patches may be chosen to be 1 mm wide ($\approx 3w_{opt}$) to reduce their number and the spatial resolution will increase to 1.7 arc seconds, dominated by the patch size (as opposed to patch diffraction).

While a detailed study has not been done, it is likely that the patch length, which plays a role analogous to the in-plane scatter in a reflective X-ray optic, can be ≈ 5 times the width and still maintain much of the system resolution. Data analysis techniques will make use of the well-defined circular PSF of the slightly defocussed (detuned) image, Figure 6(b). The half-power diameter is, however, determined by the patch length and here it would be a little over 4 arc seconds.

The spectral resolving power in general is defined as $E/dE = \lambda/d\lambda$ where $dE, d\lambda$ are the FWHM of the PSF.

For the patched diffractive optic we can ask what $d\lambda$ corresponds to a blur of size w_{image} :

$$d\lambda \approx \frac{\lambda_0}{D/2} w_{image} = \frac{\lambda_0}{D/2} \sqrt{D p_0} \quad (8)$$

which gives the resolving power of:

$$\frac{\lambda_0}{d\lambda} \approx \frac{1}{2} \sqrt{\frac{D}{p_0}}. \quad (9)$$

For the nominal parameters and optimum patch size this is $\lambda/d\lambda \approx 1200$ and would be about half this value for the $3w_{opt}$ -sized patches. This calculation also sets the period accuracy requirements for the grating patches - in this case no more stringent than for the HETG instrument.

The “roll” alignment of the patches that is needed to support these resolutions is of order $2w_{image}/D$, or about 3 arc minutes which again compares well with the HETG alignment errors of order 1 arc minute rms.

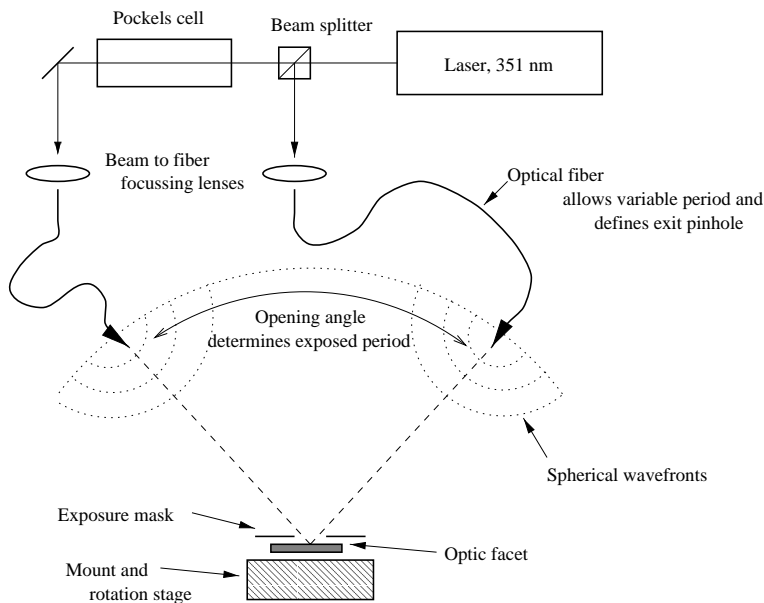


Figure 7: *Variable-period holography exposure scheme. Optical fibers are used to define the interfering beams for holography. Because of the fibers’ flexibility the system can be reconfigured for different periods in a matter of seconds.*

4.3 Fabrication of Grating Facets with patches

While the focus of this paper is not the fabrication of these patched grating facets, it is useful to discuss the general techniques that could be used. Electron-beam (“e-beam”) systems might be used to write the desired pattern, however, the scan time of these systems (minutes to write a 0.1 mm diameter zone plate¹¹) would require months to write a 25 mm by 25 mm grating facet.

Current holography systems can easily create parallel constant period gratings to the accuracies needed for each patch. Two important technological developments for patch fabrication are i) the masking of each holography exposure to a $\approx 1 \text{ mm} \times 5 \text{ mm}$ region without introducing ghosts or other scattered-light artifacts, and ii) the ability to change the period and angle of the holography exposure. This latter may be accomplished by using fiber optics to allow a range of motion of the holography sources without the need for tedious re-alignment, Figure 7. The design presented here uses grating patches with periods in the range 280 nm to 200 nm; a range well-proven with the AXAF HETG.

4.4 Focal-plane Detector and Background

Because of the long focal lengths the plate scale is of order 2 arc seconds per mm with image scales of order 1 mm. A variety of detectors could be used including CCDs, micro-channel plates, micro-calorimeters, and 2-D imaging proportional counters.

At first glance a CCD detector with 25 micron pixels seems un-matched to this system. On the other hand a single 1024×1024 CCD would provide 25×25 resolution elements which may be much harder to get in, say, a micro-calorimeter array device. Spreading the events over $\approx 40 \times 40$ pixels will relax calibration demands and reduce pixel pile-up for even the brightest sources.

By using reflection from a multi-layer all but the in-focus photons would be excluded and the system could produce truly narrow-band images.¹⁷ In this case the detector could even be a microchannel plate system.

There are two sources of “background” when doing imaging in a spectral line i) the source continuum radiation and ii) other non-source events. The large F number of the system makes the non-source background an important consideration. To assess the source continuum “background” the simulation that follows uses a realistic astrophysical plasma source spectrum.

5 RAY-TRACE SIMULATION

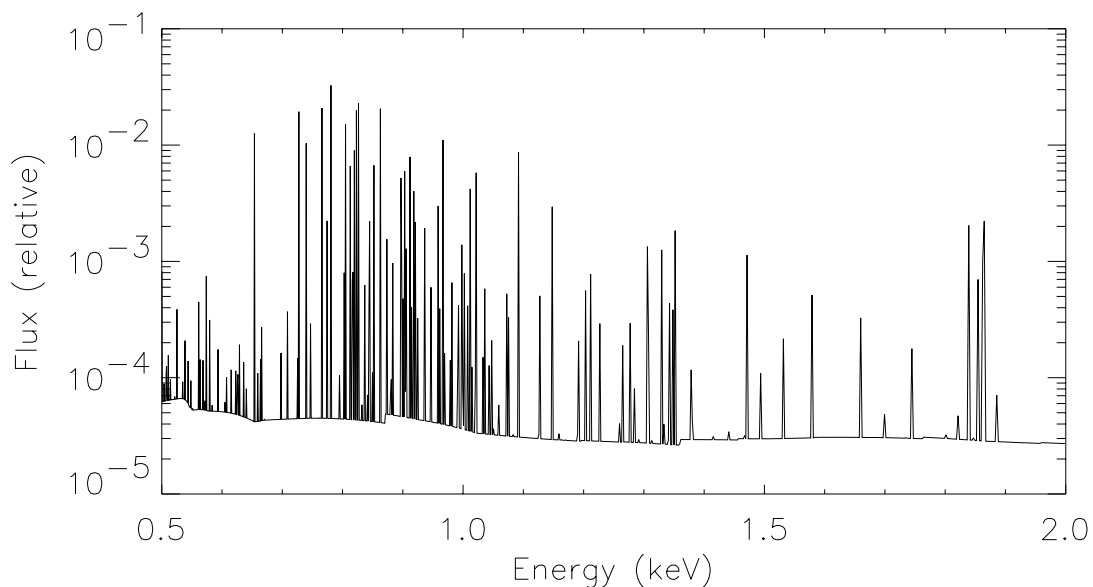


Figure 8: *Spectrum of an astrophysical-plasma source ($T = 10^{6.8} K$) multiplied by the optic effective area.*

The design described here was simulated by combining custom routines with the IRT (Interactive RayTrace from Parsec Technology Inc., Boulder, CO) package running in IDL (from Research Systems Inc.). The source is an annular ring of diameter 2 arc minutes and has the X-ray spectrum of a non-equilibrium plasma emission model, Figure 8.

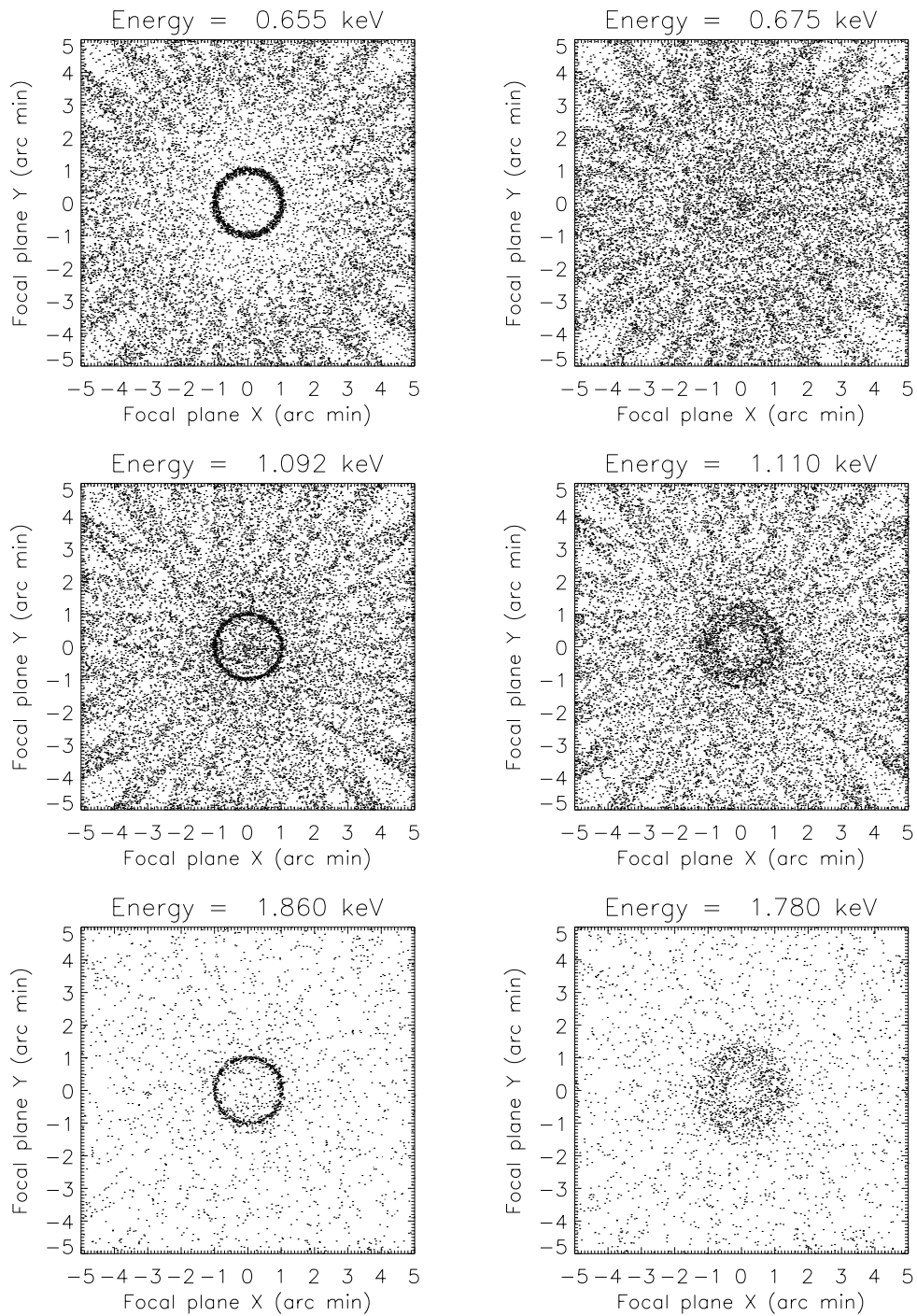


Figure 9: *Simulated narrow-band images. The source is a 2 arc minute diameter ring of X-ray emission with the spectrum shown in Figure 8. As the detector-optic distance is varied different wavelengths come into focus. The panels on the left show images when the system is tuned to an emission line and the panels on the right are for the system tuned to continuum-only regions.*

The system is able to image the ring object as the detector is moved to bring into focus the various emission lines. Because of the high angular and spectral resolving power of the instrument the line images are clearly visible, Figure 9.

6 FUTURE PROSPECTS

It is our “hunch” that there is potential for the use of diffractive optics in X-ray astronomy. Further work needs to be done in diffractive optic fabrication, system modeling, and data analysis techniques to fully realize the diffractive optic design. Optic fabrication issues focus around i) the ability to fabricate zone-plate-approximating gratings and ii) the ability to make (tilt-)blazed transmission-grating structures. Future systems may reduce the grating period, p_0 , to as fine as 100 nm to 50 nm. Higher fidelity and more realistic simulations of the instrument are needed to evaluate issues of background and deconvolution. Data analysis methods for the coupled spatial-spectral images resulting from a diffractive optical system are already being considered¹⁸ but much more work is needed.

7 ACKNOWLEDGEMENTS

This work was supported in part by NASA under the HETG contract NAS-38249 and the AXAF Science Center contract to the Smithsonian Astrophysical Observatory, NAS8-39073. We thank Claude Canizares for encouragement, stimulating discussions, and a supportive environment.

8 DEDICATION

The authors dedicate this paper to the memory of Brenda Parsons.

9 REFERENCES

- [1] *International Conference on Diffractive Optical Elements, Proc. SPIE*, Vol. 1574, 1991.
- [2] *Diffractive and Holographic Optics Technology, Proc. SPIE*, Vol. 2152, 1994.
- [3] *Diffractive and Holographic Optics Technology II, Proc. SPIE*, Vol. 2404, 1995.
- [4] G. Blough and G.M. Morris, “Hybrid lenses offer high performance at low cost”, *Laser Focus World*, pp. 67-74, November, 1995.
- [5] T.H. Markert, C.R. Canizares, D. Dewey, M. McGuirk, C.S. Pak, and M.L. Schattenburg, “High-Energy Transmission Grating Spectrometer for the Advanced X-ray Astrophysics Facility (AXAF)”, in *EUV, X-ray, and Gamma-Ray Instrumentation for Astronomy V, Proc. SPIE*, Vol. 2280, pp. 168-180, 1994.
- [6] E. Spiller, *Soft X-Ray Optics*, SPIE Optical Engineering Press, Washington, 1994.
- [7] G. Weinberg, *The Secrets of Consulting*, Dorset House Publishing, NY, 1985.
- [8] P.J. Serlemittos, et al., “The X-Ray Telescope with ASCA”, *Publ. Astron. Soc. Japan*, 47, p.105, 1995.

- [9] M.L. Schattenburg, R.J. Aucoin, R.C. Fleming, I. Plotnik, J. Porter, and H.I. Smith, "Fabrication of High Energy X-ray Transmission Gratings for AXAF", in *EUV, X-ray, and Gamma-Ray Instrumentation for Astronomy V*, *Proc. SPIE*, Vol. 2280, pp. 181-190, 1994.
- [10] R.W. Wood, "Phase-Reversal Zone-Plates, and Diffraction Telescopes", *Phil. Mag.* Series 5, Vol.45, No. 277, pp. 511-522, 1898.
- [11] A. Michette, "Diffractive optics for X-rays - the state of the art", in *International Colloquium on Diffractive Optical Elements*, *Proc. SPIE*, Vol. 1574, pp. 8-21, 1991.
- [12] O.E. Meyers, Jr., "Studies of Transmission Zone Plates", in *Selected Papers on Holographic and Diffractive Lenses and Mirrors*, T.W. Stone and B.J. Thompson, *Editors*, SPIE Milestone Series Volume MS 34, 1991.
- [13] M. Born and E. Wolf, *Principles of Optics, Sixth Ed.*, pp. 401-407., Pergamon, New York, 1980.
- [14] T.H. Markert, D. Dewey, J.E. Davis, K.A. Flanagan, D.E. Graessle, J.M. Bauer, and C.S. Nelson, "Modeling the Diffraction Efficiencies of the AXAF High Energy Transmission Gratings", in *EUV, X-Ray, and Gamma-Ray Instrumentation for Astronomy VI*, *Proc. SPIE*, Vol. 2518, pp. 424-437, 1995.
- [15] D.W. Prather, M.S. Mitroznik, and J.N. Mait, "Boundary Element Method for Vector Modelling Diffractive Optical Elements", in *Diffractive and Holographic Optics Technology II*, *Proc. SPIE*, Vol. 2404, pp.28-39, 1995.
- [16] D.A. Buralli and G.M. Morris, "Design of two- and three-element diffractive Keplerian telescopes", *Applied Optics*, Vol. 31, No.1, pp.38-43, 1992.
- [17] H.L. Marshall, private suggestion, 1996.
- [18] D. Lyons, "Image Spectrometry with a Diffractive Optic", in *Imaging Spectrometry*, *Proc. SPIE*, Vol. 2480, pp. 123-131, 1995.